Graph-Theoretical Analysis Reveals Disrupted Small-World Organization of Cortical Thickness Correlation Networks in Temporal Lobe Epilepsy

Boris C. Bernhardt[1], Zhang Chen[1], Yong He[2], Alan C. Evans[1] and Neda Bernasconi[1]

[1]Department of Neurology and Neurosurgery and McConnell Brain Imaging Center, Montreal Neurological Institute and Hospital, McGill University, Montreal, Quebec, Canada H3A 2B4 and and [2]State Key Laboratory of Cognitive Neuroscience and Learning, Beijing Normal University, Beijing, China

Address correspondence to Dr Neda Bernasconi, Montreal Neurological Institute and Hospital, McGill University, 3801 University Street, Montreal, Quebec, Canada H3A 2B4. Email: neda@bic.mni.mcgill.ca.

Temporal lobe epilepsy (TLE) is the most common drug-resistant epilepsy in adults. As morphometric studies have shown widespread structural damage in TLE, this condition is often referred to as a system disorder with disrupted structural networks. Studies based on univariate statistical comparisons can only indirectly test such hypothesis. Graph theory provides a new approach to formally analyze large-scale networks. Using graph-theoretical analysis of magnetic resonance imaging–based cortical thickness correlations, we investigated the structural basis of the organization of such networks in 122 TLE patients and 47 age- and sex-matched healthy controls. Networks in patients and controls were characterized by a short path length between anatomical regions and a high degree of clustering, suggestive of a small-world topology. However, compared with controls, patients showed increased path length and clustering, altered distribution of network hubs, and higher vulnerability to targeted attacks, suggesting a reorganization of cortical thickness correlation networks. Longitudinal analysis demonstrated that network alterations intensify over time. Bootstrap simulations showed high reproducibility of network parameters across random subsamplings, indicating that altered network topology in TLE is a consistent finding. Increased network disruption was associated with unfavorable postoperative seizure outcome, implying adverse effects of epileptogenesis on large-scale network organization.

Keywords: cortical thickness, epilepsy, graph theory, small-world networks

Introduction

Temporal lobe epilepsy (TLE) is the most common drug-resistant epilepsy in adults. Although hippocampal atrophy is the hallmark of this disorder (Cascino et al. 1991), abundant magnetic resonance imaging (MRI)-based analyses of gray matter including volumetry, voxel-based morphometry, and cortical thickness measurement have shown that structural changes extend to temporolimbic and frontocentral regions (Bernasconi et al. 2003; Bernhardt et al. 2008; Keller and Roberts 2008). Several studies have also highlighted marked morphological (Bernasconi et al. 2004; McMillan et al. 2004; Seidenberg et al. 2005) and microstructural (Concha et al. 2005; Yogarajah and Duncan 2008) white matter abnormalities located within and beyond the temporal lobes. Aside from static changes, there is accumulating evidence that atrophy intensifies over time, likely as a result of seizure-induced damage (Theodore and Gaillard 2002; Sutula et al. 2003; Bernhardt, Worsley, et al. 2009; Cascino 2009; Coan et al. 2009). The extensive character of structural changes may have negative impact on the results of surgery in term of seizure outcome (Ryvlin 2003; Keller et al. 2007; Bernhardt et al. 2010) and form the basis of cognitive impairments in multiple domains (Jokeit and Ebner 1999; Dow et al. 2004; Dabbs et al. 2009).

Although the widespread nature of structural damage in TLE is suggestive of a system disorder resulting in disrupted structural networks, studies based on univariate statistical morphometric comparisons can only indirectly test such hypothesis (Bernasconi et al. 2004; Bonilha et al. 2004; Bernhardt et al. 2008; McDonald, Hagler, et al. 2008). The introduction of graph-theoretical methods in brain imaging offers a formal framework to quantify topological and organizational properties of complex interconnected networks (Bullmore and Sporns 2009; Guye et al. 2010). Graph-theoretical analyses in healthy individuals across various modalities such as electrophysiology (Stam 2004; Bassett et al. 2006), functional MRI (fMRI) (Salvador et al. 2005; He, Wang, et al. 2009), and diffusion tensor imaging (DTI) (Iturria-Medina et al. 2008; Gong et al. 2009) have indicated that brain networks are neither random nor regular but characteristic of a small world. A small-world network is characterized by short path lengths between individual regions and a high degree of clustering (Watts and Strogatz 1998), an architecture that enables both the specialization and integration of distributed networks at low wiring costs (Sporns et al. 2004).

Brain networks can be defined either on the functional or on the structural level (Bullmore and Sporns 2009). While functional networks are derived from the temporal correlation of neurophysiological signals in different brain regions and illustrate brain dynamics on a system level (Friston et al. 1993), structural network construction is based on mapping the actual wiring or structural relationship between cortical regions. The gold standard to define such type of connections has been the use of anterograde and retrograde tract-tracing techniques. The invasiveness of these approaches limits their application to animal studies. Advances in neuroimaging techniques, particularly DTI tractography, have allowed the in vivo study of structural networks at a macroscopic level (Hagmann et al. 2008; Iturria-Medina et al. 2008; Gong et al. 2009). In regions with high fiber directionality, such as the deep white matter, DTI maps putative tracts that closely resemble known anatomical connections (Johansen-Berg and Behrens 2006), findings validated by comparative DTI and tracing studies in nonhuman primates (Parker et al. 2002; Dauguet et al. 2007). In the vicinity of cortical regions, on the other hand, water diffusion is generally highly isotropic (i.e., without a principal direction) since many small corticocortical fibers branch, kiss, and cross. Thus, despite the success in inferring connectivity of major deep white matter tracts, DTI-based approaches have

Table 1
Demographic and clinical data

Group	Age	Females	Seizure onset	Epilepsy duration	Surgery	Outcome (Engel Ia)	Hippocampal atrophy
Controls (n = 47)	32 ± 12 (18–66)	24	n.a.	n.a.	n.a.	n.a.	n.a.
LTLE (n = 63)	36 ± 10 (17–57)	36	15 ± 11 (0–47)	21 ± 11 (1–42)	49	26/46	52
RTLE (n = 59)	36 ± 11 (17–62)	34	16 ± 12 (0–49)	20 ± 13 (1–49)	45	24/44	51

Note: Age, seizure onset, and duration of epilepsy are presented in years ± SD (range); Engel Ia: proportion of completely seizure-free patients after surgery; n.a., not applicable.

limited validity to map corticocortical connectivity. Even if recent techniques allow circumventing some of these limitations by modeling the uncertainty of fiber direction, for example, they may on the other hand produce higher numbers of false positive tracts (Behrens et al. 2003; Parker and Alexander 2005; Gong et al. 2009). Furthermore, with regard to mapping corticocortical networks across the entire brain, a DTI-based approach may become problematic as anatomical distance between 2 cortical seed regions increase. In addition, physical properties such as curvature, the number of fibers, and alterations in tracts' microstructure in case of pathology may affect the validity of the tracing (Dauguet et al. 2007; Powell et al. 2007).

Correlation analysis of structural MRI data has been proposed as an alternative framework to study structural networks (Bullmore et al. 1998; Lerch et al. 2006; He et al. 2007; Bassett et al. 2008; Bernhardt et al. 2008). This approach rests on the assumption that positive correlations indicate connectivity, as axonally connected regions are believed to have common trophic, developmental, and maturational influences (Cheverud 1984; Wright et al. 1999; Zhang and Sejnowski 2000). MRI-based cortical thickness measurement has been proposed as a valid covariate, as it offers an index of cortical morphology that reflects the size, density, and arrangement of neurons and neuropil in a biological and topological meaningful way (Parent and Carpenter 1995). Morphometric correlations of cortical thickness data have mapped successfully structural networks that closely resembled tract-tracing data (Mitelman et al. 2005; Lerch et al. 2006; Bernhardt et al. 2008).

Graph-theoretical analyses of MRI-based thickness correlations have shown a small-world organization of the cerebral cortex in healthy individuals (He et al. 2007) and have suggested alteration of such an arrangement in Alzheimer's disease, multiple sclerosis, and schizophrenia (Bassett et al. 2008; He et al. 2008; He, Dagher, et al. 2009). The purpose of this study was to assess the structural basis of large-scale brain organization in drug-resistant TLE using graph-theoretical analysis of cortical thickness correlations. Based on the knowledge of extensive structural damage in this condition, we hypothesized that the disruption of cortical thickness correlation networks would progressively increase over time. In addition, we investigated the impact of network properties to clinically relevant parameters such as postsurgical outcome. Lastly, we assessed the reproducibility of network parameters and between-group differences using a bootstrap approach.

Materials and Methods

Subjects
We studied 122 consecutive patients with drug-resistant TLE. Demographic and clinical data were obtained through interviews with the patients and their relatives. TLE diagnosis and lateralization of the seizure focus into 63 patients with left TLE (LTLE) and 59 with right TLE (RTLE) were determined by a comprehensive evaluation including detailed history, video electroencephalography (EEG) telemetry, neuroimaging, and neuropsychological assessment in all patients. Hippocampal atrophy was determined as hippocampal volumes or an interhemispheric hippocampal asymmetry beyond 2 standard deviation (SD) of the corresponding mean of healthy controls (Bernasconi et al. 2003). None of the patients had any other lesions visible on MRI or a history of traumatic brain injury.

For those 94 patients who underwent surgery, we assessed surgical outcome according to Engel's modified classification scheme (Engel et al. 1993). Four patients were lost for follow-up. Due to subpial aspiration, specimens were unsuitable for histopathology in 22 patients. In the remaining 72 samples, qualitative pathological examination (Meencke and Veith 1991) revealed hippocampal sclerosis in 58 (81%) patients.

Within our TLE population, a subset of 26 patients (9 LTLE, 17 RTLE) refused to undergo surgery at the first evaluation made by our epilepsy team. These patients, however, agreed to have repeated MRI scans. Twelve of them eventually followed our recommendation and were operated at subsequent hospitalizations. All images were acquired on the same MR scanner. The interval between the first and last scan was 27 ± 20 months (range = 4–90 months).

The control group consisted of 47 age- and sex-matched healthy individuals recruited using a set standardized subject inclusion/exclusion criteria defined by International Consortium for Brain Mapping (Mazziotta et al. 2009). The Ethics Committee of the Montreal Neurological Institute and Hospital approved the study and written informed consent was obtained from all participants. Demographic and clinical data of all subjects are shown in Table 1.

MRI Acquisition and Construction of Cortical Correlation Matrices
MR images were acquired on a 1.5-T Gyroscan (Philips Medical Systems) using a 3D T_1-fast field echo sequence (repetition time = 18 ms, echo time = 10 ms, 1 excitation, flip angle = 30°, matrix size = 256 × 256, field of view = 256 × 256 mm², slice thickness = 1 mm), providing an isotropic voxel of volume = 1 mm³. Each image underwent automated correction for intensity nonuniformity and intensity standardization (Sled et al. 1998). Images were linearly registered into a standardized stereotaxic space based on the Talairach atlas (Collins et al. 1994).

As in our previous work (Bernhardt et al. 2008), we applied the Constrained Laplacian Anatomic Segmentation using Proximity algorithm (MacDonald et al. 2000; Kim et al. 2005) to generate a model of the cortical surface and to measure cortical thickness across thousands of surface-spanning vertices in native space.

Cortical thickness correlation network construction procedures have been described previously (He et al. 2007). In short, extracted cortical surfaces were segmented into 52 anatomical regions using the ANIMAL algorithm (Collins et al. 1995). ANIMAL nonlinearly registers an individual MRI volume to an anatomically segmented atlas in a multiscale fashion. Using the inverse of this transform, atlas labels were warped back to the individual MRI and intersected with the individual surfaces. We measured the mean cortical thickness across all vertices in each anatomical region. The listing of the anatomical regions is given in Supplementary Table 1. Cortical thickness data were statistically corrected for age, gender, and overall mean cortical thickness. For each group, an interregional correlation matrix R of

52 × 52 dimensions was generated, where an individual entry r_{ij} contained the Pearson product moment cross-correlation coefficients of the mean cortical thickness across subjects in regions i and j.

In a separate analysis, cortical surfaces were segmented using automated anatomical labeling (AAL) as an alternative parcellation scheme that divides the cortex into approximate Brodmann areas (Tzourio-Mazoyer et al. 2002).

Network Topology Analysis
The absolute of the correlation coefficient matrix R was thresholded into a binarized connectivity matrix A, where an entry a_{ij} equals 1 if $|r_{ij}|$ exceeded a given threshold and 0 otherwise. Nonzero entries in A correspond to connections between 2 anatomical regions. Such a binary 52 × 52 matrix is thus equivalent to an undirected graph with 52 nodes (i.e., regions) and $K/2$ edges (i.e., connections), where K is the total number of nonzero entries. Diagonal elements in A were set to 0.

The density of a network with n nodes was defined as the percentage of the total number of connections K divided by the number of possible connections, that is, density = $K/(52 \times 51) \times 100\%$. Similar to previous work on the cortical thickness correlation network in Alzheimer's disease (He et al. 2008), group comparisons were performed after thresholding individual correlation matrices of controls, LTLE, and RTLE at a fixed network density. This procedure ensured that networks in all groups have the same number of edges or wiring cost (Achard and Bullmore 2007) and that the between-group differences reflected alterations in topological organization rather than differences in low-level correlations (He et al. 2008).

Small-World Analysis
We computed the clustering coefficient C, the characteristic path length L, and the small-world index σ in controls, LTLE, and RTLE over a wide range of network density thresholds (5–40%). The range of densities was chosen to allow a proper estimation of small-world parameters while minimizing the number of spurious edges in each network (Achard and Bullmore 2007; He et al. 2008).

The clustering coefficient c_i of a node i was defined as (Watts and Strogatz 1998):

$$c_i = \frac{E_i}{\frac{k_i(k_i - 1)}{2}}.$$

E_i is the number of existing connections among the neighbors of node i. As k_i is the actual number of neighbors of node i (i.e., its degree), the denominator term $k_i(k_i - 1)/2$ quantifies the number of all possible connections among the neighboring nodes. If a node i had only one edge or no edges, c_i was set to 0. The clustering coefficient C of a network was then defined as the mean clustering coefficient over all nodes in the network:

$$C = \frac{1}{n} \sum_{i=1}^{n} c_i.$$

C thus quantifies the cliquishness and is related to the local efficiency of a network (Latora and Marchiori 2001).

The characteristic path length l_i of a node i was defined as (Watts and Strogatz 1998):

$$l_i = \frac{1}{n-1} \sum_{i \neq j} \min\{l_{ij}\}.$$

Here, $\min\{l_{ij}\}$ is the shortest absolute path length between the node i and j. The characteristic path length L of a network was then defined as the mean minimum number of edges that lies between any 2 nodes in the network. To overcome the problem of dramatically increased L values in networks with possibly disconnected components, L was calculated using the harmonic mean definition (Newman 2003; He et al. 2008):

$$L = \frac{n}{\sum_{i=1}^{n} \frac{1}{l_i}}.$$

The reciprocal of L is a measure of parallel information transfer or global efficiency of a network (Latora and Marchiori 2001).

Compared with random networks, small-world networks have similar characteristic path lengths, but higher clustering, that is $\gamma = C/C_{rand} > 1$ while $\lambda = L/L_{rand} \approx 1$ (Watts and Strogatz 1998). The small-world index $\sigma = \gamma/\lambda$ is thus greater than 1 in small-world networks (Humphries et al. 2006; Humphries and Gurney 2008). C_{rand} and L_{rand} were defined as the mean clustering coefficient across 1000 randomly generated networks that had the same number of nodes, edges, and degree distribution as the real network (Maslov and Sneppen 2002; Sporns and Zwi 2004).

Network Robustness Analysis
Network robustness, characterized by the degree of tolerance against random failures and targeted attacks, is usually associated with the stability of a complex network. Cortical thickness correlation networks were constructed at a density of 15%. This was the lowest threshold that guaranteed that all anatomical regions in LTLE, RTLE, and controls were included in the networks (i.e., any pair of nodes is connected through a series of edges), thus minimizing the number of false positive paths (He et al. 2008). Such a fixed constraint optimizes interregional correlation strength and therefore is biologically plausible (Bassett and Bullmore 2006).

In the "random failure analysis," we successively removed randomly chosen nodes of the network in each group and assessed the relative size of the remaining largest connected component. The same analysis was performed on the edges of the network. Each analysis was repeated 1000 times, and the mean relative size of the largest connected component was computed.

In the "targeted attack analysis," we removed nodes in decreasing order of their network betweenness centrality. The betweenness centrality of a node i was defined as the number of shortest paths between any 2 nodes in the network that pass through i. It thus captures the influence of a node on information flow in the network, especially when network information flow tends to follow the shortest paths (Freeman 1977; Girvan and Newman 2002). We normalized betweenness centrality of each node by dividing it by the mean betweenness centrality across all nodes. We used the MatlabBGL package (http://www.stanford.edu/~dgleich/programs/matlab_bgl/) to compute the betweenness centrality of each node. The same analysis was also performed on the edges of the network. The betweenness centrality of an edge e was defined as the number of shortest paths between any 2 nodes in the network that pass through e (Girvan and Newman 2002).

Mapping of Degree Distribution and Hub Regions
Within each group (controls, LTLE, RTLE), we mapped the connectivity degree distribution of the network. We defined hub regions as those with a nodal betweenness centrality that was 1 SD above the mean nodal betweenness centrality of all cortical regions. Hub regions were classified into primary, association, and paralimbic areas (Mesulam 1998).

Statistical Analysis
Differences in network parameters C, L, γ, λ, and σ as well as network robustness measures were assessed separately between each TLE group (i.e., LTLE, RTLE) and controls using a nonparametric permutation test with 1000 repetitions (Bullmore et al. 1999). In each randomization procedure, cortical thickness data of each subject were randomly reassigned to 1 of the 2 groups. We then obtained connectivity matrices, network parameters, and network robustness measures in each randomized group and calculated their differences. This generated a permutation distribution of differences under the null hypothesis. The true between-group difference was then placed in its corresponding permutation distribution. Its percentile position yielded the significance level of a 2-tailed group difference between each TLE group and controls. As in previous work (He et al. 2008), significances were thresholded at $P < 0.05$.

Relation to Surgical Outcome
We separated our TLE groups into those with a seizure-free (Engel class Ia) and non–seizure-free (Engel class Ib-IV) surgical outcome. Analogous to the above analysis, we obtained cortical thickness

correlation matrices in both subgroups and compared network parameters using permutation methods.

Longitudinal Analysis

To assess progressive changes in network organization in our TLE patients with longitudinal data ($n = 26$), we obtained cortical thickness correlation matrices at baseline and follow-up scans and calculated the network parameters. Permutation tests were performed using within-subject randomization.

Reproducibility Analysis

Cross-Sectional Data sets

We estimated the confidence intervals of network parameters C, L, γ, λ, and σ in controls, LTLE, and RTLE using a bootstrap approach with 1000 randomizations. In sampling with replacement, after randomly drawing an individual from the original sample, this individual is put back before drawing the next one. Each resample had the same size as the original sample (i.e., $n = 63$ for LTLE, $n = 59$ for RTLE, and $n = 47$ for controls).

Longitudinal Data set

To assess whether the longitudinal subset was representative of the overall TLE sample, we placed its network parameters at baseline into distributions generated by 1000 random draws of 26 patients from the overall sample. In each randomization, the ratio of LTLE/RTLE was preserved.

In each randomization of the cross-sectional and longitudinal datasets, it was ensured that the bootstrapped networks were fully connected.

Results

Cross-Sectional Analysis

Interregional Cortical Thickness Correlations in Controls, LTLE, and RTLE

Interregional cortical thickness correlation matrices, connectivity matrices, and connectivity graphs are shown in Figure 1. Correlation matrices in the 3 groups exhibited similar patterns, with generally strong correlations between bilaterally homologous regions and strong correlations between regions within the same lobe. However, compared with controls, overall mean strength of positive correlations in LTLE and RTLE was increased while the mean strength of negative correlations was decreased ($t > 4.5$, $P < 0.005$).

Cortical Thickness Correlation Network Topology in TLE

Network parameters of controls, LTLE, and RTLE are presented in Table 2.

In all 3 groups, that is, controls, LTLE, and RTLE, we observed a small-world index σ greater than 1 over the entire range of density thresholds. This was reflected in $\gamma = C/C_{rand} > 1$ and $\lambda = L/L_{rand} \approx 1$, indicating a small-world organization in both patient and control groups (Supplementary Fig. 1). Indeed, comparing σ, γ, and λ between controls and TLE did not yield a significant difference.

Comparing patients with controls, we observed increased clustering coefficients in both TLE groups over almost the entire range of density thresholds (Fig. 2A). Hence, mean clustering across all densities (5–40%) was increased in both TLE groups compared with controls ($P < 0.03$, Supplementary Fig. 2A).

Comparing patients with controls, we found trends for increased path length over several density thresholds in both TLE groups (Fig. 2B). While there was only a trend for an increase in mean path length across all densities (5–40%) in

LTLE ($P = 0.12$), this increase was significant in RTLE ($P < 0.05$, Supplementary Fig. 2B).

Tendencies for increased clustering and path length were seen when a more restricted density range (15–25%) was chosen. This 'small-world range' (Bassett et al. 2008) guaranteed fully interconnected networks as well as a small-world index $\sigma > 1.2$. Moreover, we observed comparable degrees of network alterations in TLE patients when using the AAL parcellation algorithm (Tzourio-Mazoyer et al. 2002).

In a separate analysis, we constructed networks in controls and TLE groups also on the basis of absolute correlation strength. While the density-based thresholding employed in our main analysis guaranteed an equal number of connections across groups and thus allowed us to compare topological properties of cortical thickness correlation networks unaffected by differences in low-level correlations, network threshold based on absolute correlation strength may give a more straightforward interpretation of a connection as representing a correlation exceeding a given value (chosen from $|r| = 0.05 - 0.4$). In patients, such networks also showed a tendency for increased clustering relative to networks in controls ($P < 0.057$). On the other hand, we could not reproduce the tendencies for increased path length that were observed using density-based thresholding ($P > 0.4$).

Degree distribution and hub regions: In both controls and patients, we observed that the connectivity degree distribution included mostly nodes with relatively few connections and some nodes with many connections. An exponentially truncated power law moderately modeled this degree distribution (Supplementary Fig. 3); however, we observed a smaller proportion of nodes with excessive connections than expected from the fit. Although results are presented for a density of 15%, similar degree distributions were consistently observed across density thresholds from 5% to 40%.

In healthy controls, 7 hubs were seen in association and 1 in primary cortices. In patients, the distribution of hubs was somewhat different than in controls. In LTLE, 2/10 hubs were seen in paralimbic and 3 hubs in primary areas. Three of the 5 hubs in the association areas were located in temporal and supramarginal cortices. In RTLE, 1 hub was seen in paralimbic and 5 in association areas, with 4 of them in temporal and angular cortices (Table 3).

Network Robustness Analysis

While networks in TLE patients were globally as robust to random node failures and random edge failures as those in healthy controls, they were more vulnerable to targeted node and edge attacks (Fig. 3).

Targeted node attacks led to significant network breakdowns ($P < 0.05$) across almost the entire range of removed nodes in both LTLE and RTLE. Overall, networks were more vulnerable to targeted attacks in both TLE groups relative to controls (difference in area under the curve: $P < 0.05$). Comparable findings were also observed in the targeted edge attacks analysis, with an overall increased vulnerability in both patient groups (difference in area under the curve: $P < 0.05$).

In the random failure analysis, we did not observe any differences in overall network robustness (no difference in area under the curve: $P > 0.1$) between patients and controls.

Although results are reported for networks at a fixed density of 15% (i.e., the minimal threshold at which all networks are fully connected), patterns of findings from the network

Cortical thickness correlation networks in the cross-sectional cohorts

A) Healthy controls

B) LTLE

C) RTLE

correlation matrix **connectivity matrix** **connectivity graph**

correlation coefficient: 1 to -1

no connection / connection
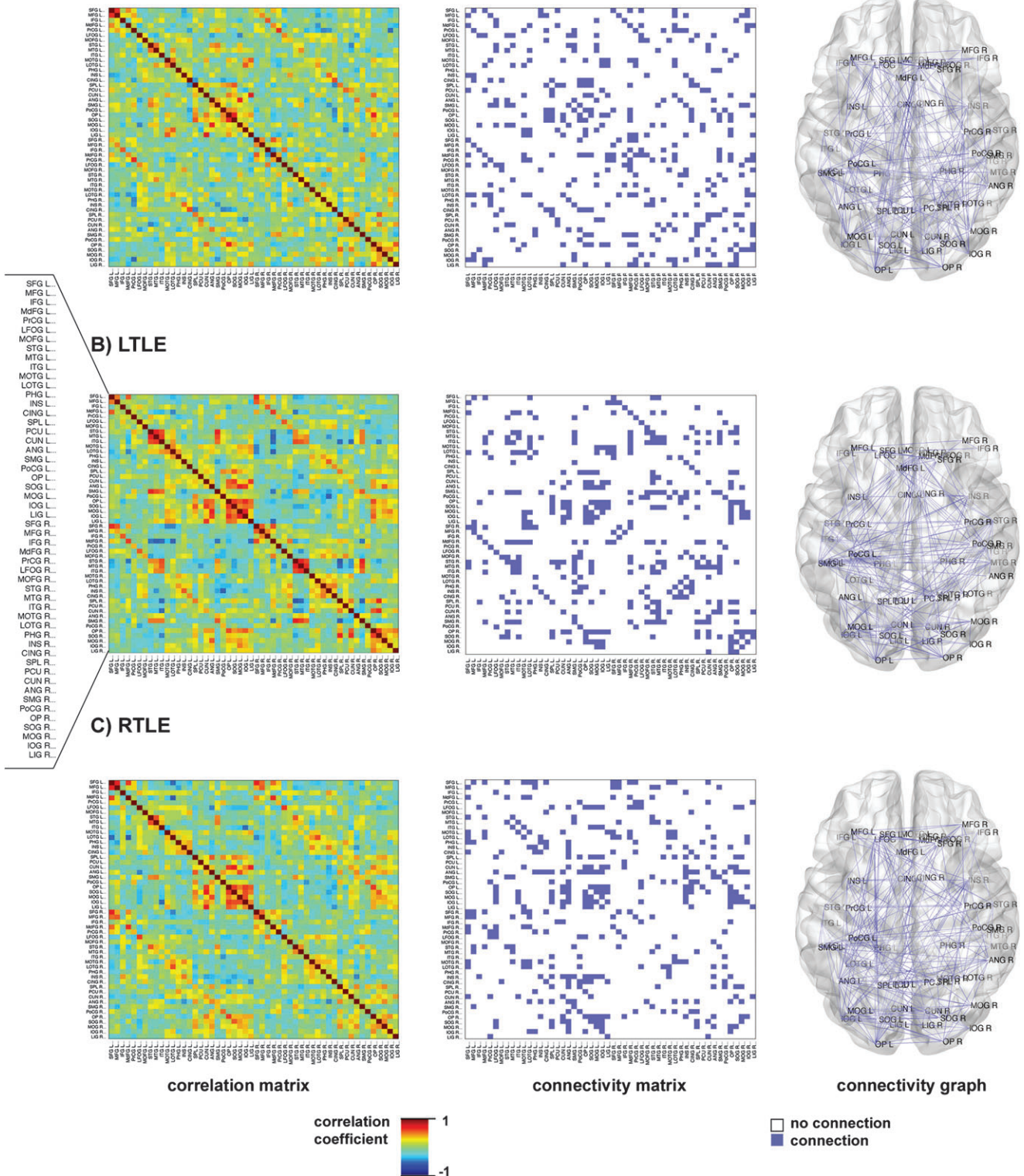
Figure 1. Cortical thickness correlation networks in (*A*) healthy controls, (*B*) LTLE, and (*C*) RTLE. The left column displays the cortical thickness correlation matrices of 52 anatomical areas. The middle column displays the binary connectivity matrices thresholded at a fixed network density of 15%. The right column illustrates the corresponding brain connectivity graph seen from above. For anatomical abbreviations, please see Supplementary Table 1.

Table 2

Network parameters in the cross-sectional sample

Parameter	Controls ($n = 47$)	LTLE ($n = 63$)	RTLE ($n = 59$)
L	1.94	2.02	1.99
λ	1.03	1.06	1.04
C	0.31	0.42	0.38
γ	1.84	1.81	1.93
σ	1.79	1.71	1.86

Note: Results are reported at 15% network density (the minimal threshold where original networks were fully connected). As there exists only one value for each group, there are no standard errors reported with these values. L, mean shortest path length; C, clustering coefficient; λ, γ, σ are small-world parameters. Note that $\gamma > 1$, $\lambda \approx 1$, and $\sigma > 1$ in small-world networks.
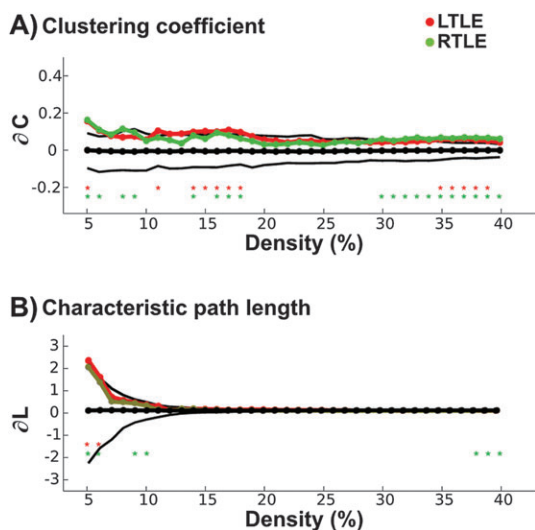
Figure 2. Network parameter analysis of the cross-sectional cohort. The colored lines show differences (δ) between each TLE group and controls for clustering coefficient (A, δC) and characteristic path length (B, δL) as a function of network density. While $\delta = 0$ indicates no difference, $\delta > 0/\delta < 0$ indicates an increase/decrease in the network density of TLE patients relative to controls. The black lines show the mean and 95% confidence interval of the null distribution of no between-group difference obtained from 1000 permutation tests at each density value (only displayed for LTLE). Stars indicate significant between-group differences ($P < 0.05$).

robustness analysis were relatively consistent across network density thresholds from 5% to 25%. At higher network density thresholds, all groups were generally more robust against failures and attacks.

Relationship between Presurgical Network Impairment and Postsurgical Outcome

We found a trend for increased clustering ($P = 0.1$) and path length ($P < 0.06$) across all density thresholds in non seizure-free patients (class Ib–IV) relative to those with seizure-free outcome (class Ia, Fig. 4). Effects were similar when LTLE and RTLE were considered separately and when a more restricted (15–25%) density range was chosen.

Longitudinal Analysis

The comparison of the network at follow-up to baseline scans revealed increased path length at follow-up over almost the entire range of density thresholds (Fig. 5), leading to an increased area of under the curve ($P < 0.03$). Clustering, on the other hand, did not differ between baseline and follow-up ($P = 0.4$).

Table 3

Regions of high betweenness centrality relative to random networks

Region	NB	Degree	Class
Controls			
Right medial frontal	3.14	17	Association
Right lateral temporooccipital	2.48	14	Association
Right superior occipital	2.47	8	Association
Right angular	2.39	10	Association
Right lingual	2.32	13	Association
Right cuneus	2.17	9	Association
Left supramarginal	2.14	10	Association
Right precentral	1.81	13	Primary
Left supramarginal	3.03	15	Association
LTLE			
Right middle temporal	2.97	14	Association
Right medial frontal	2.79	16	Association
Left occipital pole	2.40	13	Primary
Right insular	2.39	9	Paralimbic
Right superior temporal	2.31	17	Association
Right medial frontoorbital	2.15	10	Paralimbic
Right superior parietal	2.07	14	Association
Left postcentral	1.99	7	Primary
Right occipital pole	1.94	15	Primary
RTLE			
Left superior frontal	3.46	14	Association
Left angular	3.42	19	Association
Right insular	2.87	13	Paralimbic
Right angular	2.85	11	Association
Right lateral temporooccipital	2.10	10	Association
Right medial temporooccipital	2.06	8	Association

Note: NB, normalized betweenness centrality; degree, number of connections. Cortical regions were classified into primary, association, and paralimbic areas (Mesulam 1998).

Reliability and Reproducibility of Network Metrics

Cross-Sectional Cohorts

Bootstrapped network parameters across 1000 random subsamples (Supplementary Table 2) were distributed closely to the same parameters in the original sample of controls and TLE patients (see Table 2). The boundaries of the bootstrap intervals confirmed increased clustering and path length in patients. Indeed, when comparing the mean clustering and path length (across 5–40% density) between each randomly chosen TLE and control group, we observed increased clustering and path length in more than 99% of 1000 resamplings.

Longitudinal Cohort

Network parameters of the longitudinal subsample fell well within bootstrapped confidence intervals generated by randomly subsampling 26 patients from the total sample (Supplementary Table 3), indicating that the longitudinal group was representative of the overall TLE population.

Discussion

We performed graph-theoretical analysis on MR-based cortical thickness correlations and compared the small-world properties of large-scale structural networks in healthy controls and patients with drug-resistant TLE. Compared with univariate mapping of pathology performed in our previous analyses of cortical thickness (Bernhardt et al. 2008; Bernhardt, Rozen, et al. 2009; Bernhardt, Worsley, et al. 2009; Bernhardt et al. 2010), this approach more specifically addresses the network organization underlying whole-brain pathological interactions in TLE.
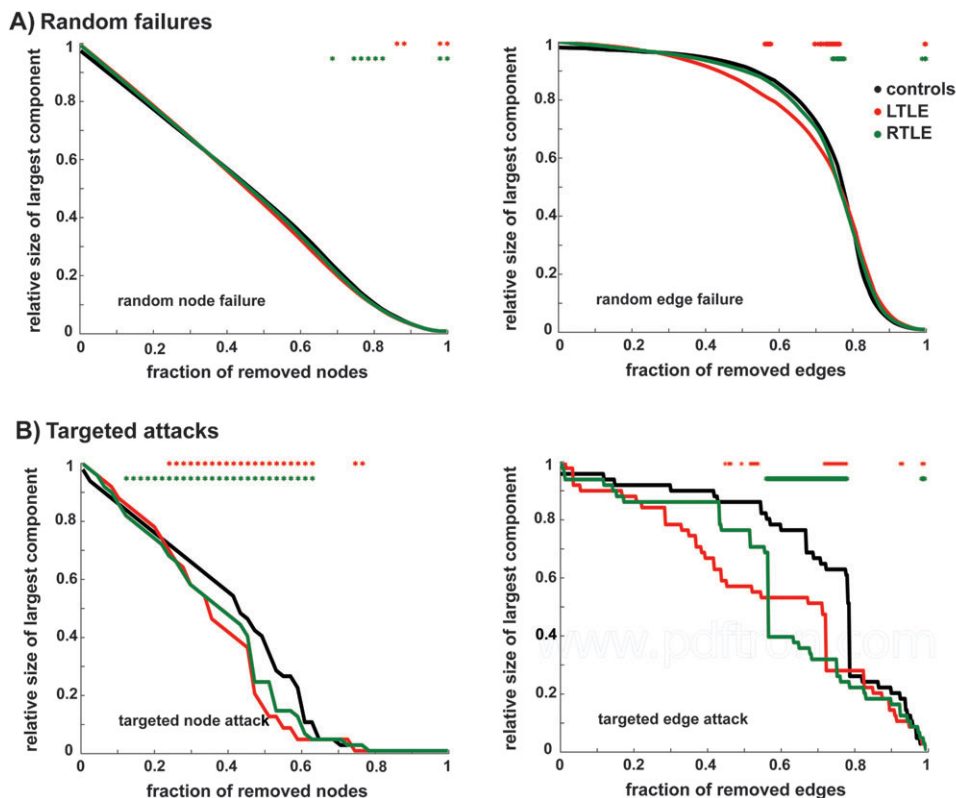
Figure 3. Network robustness analysis. Graphs display the relative size of the largest connected component (i.e., the largest subnetwork of nodes that are mutually reachable) as a fraction of removed nodes (left panels) and edges (right panels) by (*A*) random failures and (*B*) targeted attacks. Stars indicate differences ($P < 0.05$) between groups obtained from 1000 permutation tests at each density value.

Cortical thickness correlation networks in our healthy controls and patients exhibited a higher clustering but similar path length compared with corresponding random networks across a wide range of network densities, suggestive of a small-world topology. The degree distributions in all 3 groups indicated that these networks included mostly nodes with few connections, together with some nodes with many connections. These findings are in line with data from previous graph-theoretical analyses of structural networks that were derived from DTI tractography and cortical thickness correlations that have suggested a truncated power-law distribution of the connectivity degree in brain networks of healthy subjects (He et al. 2007, 2008; Bassett et al. 2008; Iturria-Medina et al. 2008; Bullmore and Sporns 2009; Gong et al. 2009; Guye et al. 2010). Group analysis of clustering and path length between healthy controls and patients, however, revealed increases in the latter. Moreover, networks of patients were more vulnerable to targeted attacks. These results suggest an altered topology of cortical thickness correlation networks in patients with TLE. Our longitudinal analysis revealed that network alterations intensify over time. Assessing the relationship between network organization on preoperative MRI and postsurgical outcome, we found trends for more severe network alterations in patients who continued to have seizures after surgery.

Altered Topology of Cortical Thickness Correlation Networks in TLE: Neurobiological Considerations

We have previously used MRI-based cortical thickness correlations to map specific networks such as entorhinal and thalamocortical circuitry in healthy individuals and patients with epilepsy (Lerch et al. 2006; Bernhardt et al. 2008; Bernhardt, Rozen, et al. 2009). In TLE, we found local interregional network disruptions between the entorhinal cortex and the neocortex (Bernhardt et al. 2008). The comparison of global network organization of patients to controls performed in the current study revealed increased path length and clustering in TLE that were consistently present over a wide range of network thresholds. Thus, although small-world topological characteristics were preserved in patients (as confirmed by $\gamma = C/C_{\mathrm{rand}} > 1$ and $\lambda = L/L_{\mathrm{rand}} \approx 1$ over the entire range of network densities and the absence of between-group differences in these parameters), our data suggest that structural networks in TLE may show subtle topological alterations, with a more regularized or lattice-like configuration (i.e., with high C and L values) than healthy controls. The patterns of network disruptions in our patients were similar using 2 different anatomical parcellations schemes (Collins et al. 1995; Tzourio-Mazoyer et al. 2002).

Further confidence in our findings was provided by the bootstrap analysis. We observed that across hundreds of random subsamplings, the confidence intervals of network parameters remained relatively tight and similar to the parameters seen in the original groups, suggesting a high reproducibility across subgroups of patients and controls. Moreover, increased clustering and path length in TLE relative to controls were observed in more than 99% of all resamplings, supporting that altered network topology is a consistent finding in TLE.

A more regularized network configuration may reduce its resilience to pathological attacks (Achard and Bullmore 2007).

A) Clustering coefficient
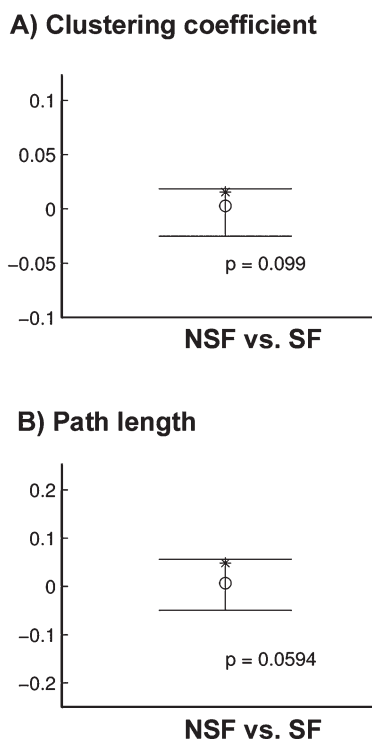
B) Path length

Figure 4. Relationship between network alterations and seizure outcome after surgery. The stars indicate the observed difference in area under the curve of the path length (*A*) and clustering coefficient (*B*) between non seizure-free (NSF) and seizure-free (SF) patients. The circle indicates the mean and the error bars indicate the 95% confidence interval of the null distribution of no between-group difference obtained from 1000 permutation tests.

A) Clustering coefficient

B) Characteristic path length
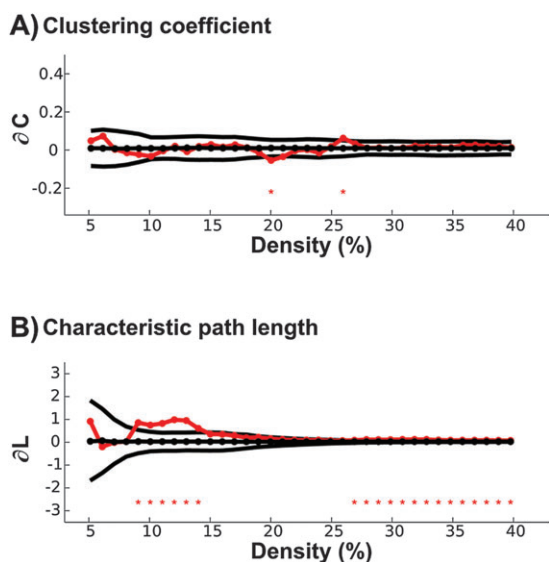
Figure 5. Network parameter analysis of the longitudinal cohort. The colored lines show the difference (δ) in clustering coefficient (*A*, δ*C*) and characteristic path length (*B*, δ*L*) between baseline and follow-up networks as a function of network density. While δ = 0 indicates no difference, δ > 0/δ < 0 indicates an increase/decrease in the network at follow-up relative to baseline. The black lines show the mean and 95% confidence interval of the null distribution of no difference obtained from 1000 permutation tests at each density value. Stars indicate significant between-scan differences ($P < 0.05$).

Indeed, networks in our patients demonstrated reduced tolerance against targeted edge (i.e., connections) and nodes (i.e., regions) removal. A reduced tolerance against targeted attacks may stem from a lack of potential alternative backup routes, thus indicative of impairments in the parallel organization of cortical thickness correlation networks possibly secondary to disease-related loss of tissue integrity.

We noted differences between TLE groups and controls in the distribution of hub regions with high betweeness centrality. While in controls these regions were found primarily in multimodal cortical association cortices and evenly distributed across all 4 lobes, a considerable proportion of hubs in our patients were found in paralimbic and temporal association cortices. It is tempting to speculate that the predominance of limbic hub regions in TLE may be related to disturbed connectivity between temporolimbic and extratemporal neocortical networks possibly secondary to disrupted fiber pathways, a hypothesis in line with diffusion tractography studies (Concha et al. 2005; McDonald, Ahmadi, et al. 2008; Yogarajah and Duncan 2008; Voets et al. 2009). Increased path length and clustering and altered topography of hub regions may further lead to reduced efficiency of global information transfer (Latora and Marchiori 2001) and signal propagation speed between temporolimbic and extratemporal neocortical networks (Achard and Bullmore 2007) and contribute to the decline in various cognitive domains in TLE (Hermann et al. 2009).

Clinical Implications of Altered Cortical Thickness Correlation Networks in TLE

From a practical point of view, DTI-based tractography as well as fMRI-based functional connectivity would allow the construction cortical networks on the individual subject level, a feature that may prove advantageous in the presurgical assessment of single patients compared with structural network generation based on group-wise correlations. On the other hand, network construction on the basis of T_1-weighted images that have, unlike DTI, played an essential role as standard clinical imaging in intractable epilepsy for many years allowed us to study a large consecutive cohort of patients including those who had longitudinal data.

Our longitudinal analysis demonstrated dynamic alterations of cortical thickness correlation network organization in TLE. Although only a fraction of our patients had longitudinal data available, bootstrap analysis demonstrated that their network properties fell within the expected range when randomly subsampling our cross-sectional patient sample, thereby indicating that our sample was sufficiently representative of the TLE population with pharmacoresistant epilepsy. Despite the lack of a longitudinal cohort of controls, the progressive nature of perturbed network organization closely mirror findings from previous reports on progressive atrophy in neocortical regions, which has been shown to be more marked than cross-sectional and longitudinal effects seen in controls (Bernhardt, Worsley, et al. 2009; Coan et al. 2009).

The general direction of topological alterations in large-scale networks observed in our patients closely resembles those found in graph-theoretical analyses of intracerebral EEG recordings during focal seizures (Ponten et al. 2007; Kramer et al. 2008; Schindler et al. 2008) and scalp EEG data of generalized absence seizures (Ponten et al. 2009). Analysis based on interictal EEG has provided somewhat diverging results, with a study showing a more regularized networks (i.e., with high *C* and *L*) (Horstmann et al. 2010), while another reported progressively more random (i.e., with low *C* and *L*)

topologies (van Dellen et al. 2009). Nevertheless, it is tempting to speculate that network synchronization during the ictal phase may influence mutual intercortical trophic exchanges, ultimately leading to progressive and long-lasting remodeling of interregional structural networks. In vitro simulation studies have also suggested an association between seizures, neuronal loss, and alterations in the topology of mesiotemporal networks at a cellular level (Netoff et al. 2004; Dyhrfjeld-Johnsen et al. 2007).

Our analysis showed tendencies for increased path length and clustering in patients who continued to have seizures after surgery compared with those who became seizure free. Seizure recurrence after surgery is believed at least in part to be related to a more extended epileptogenic network (Ryvlin 2003; Bartolomei et al. 2008; Bernhardt et al. 2010) that may consequently affect adversely structural network organization as shown by our results.

All interictal fMRI functional connectivity analyses in TLE except one have studied local alterations in cortical networks in TLE by statistically comparing the strength of interregional blood oxygen level–dependent signal correlations between patients and controls. These studies have shown decreased connectivity in ipsilateral temporal lobe networks together with contralateral increases (Bettus et al. 2009) and decreased connectivity in language networks at rest (Waites et al. 2006), as well as decreased connectivity between temporal and default-mode networks during functional tasks (Frings et al. 2009; Voets et al. 2009). A recent graph-theoretical analysis of resting-state fMRI in TLE showed decreased path length and clustering in TLE (Liao et al. 2010). The divergence between our study and the above-mentioned likely stems from the clinical inclusion criteria. Whereas we included patients with unilateral TLE, this study was based on 23 young (mean age 24 years) patients with electroclinical and imaging signs of bilateral TLE who have seemingly a more diffuse and severe type of epilepsy.

The cross-sectional and longitudinal small-world analyses performed in this study provide a comprehensive view on progressive reorganization of large-scale interregional structural networks, supporting that TLE indeed is a system disorder. Moreover, the graph theoretic approach lends a formal framework that would allow future studies not only to further explore higher order features such as network modularity and hierarchy (Bassett et al. 2008; Chen et al. 2008) but also to integrate structural morphometric, DTI-based as well as electrophysiological and functional data in a unified framework.

Supplementary Material

Supplementary material can be found at: http://www.cercor.oxfordjournals.org/.

Funding

Notes

References

Achard S, Bullmore E. 2007. Efficiency and cost of economical brain functional networks. PLoS Comput Biol. 3:e17.

Bartolomei F, Chauvel P, Wendling F. 2008. Epileptogenicity of brain structures in human temporal lobe epilepsy: a quantified study from intracerebral EEG. Brain. 131:1818-1830.

Bassett DS, Bullmore E. 2006. Small-world brain networks. Neuroscientist. 12:512-523.

Bassett DS, Bullmore E, Verchinski BA, Mattay VS, Weinberger DR, Meyer-Lindenberg A. 2008. Hierarchical organization of human cortical networks in health and schizophrenia. J Neurosci. 28:9239-9248.

Bassett DS, Meyer-Lindenberg A, Achard S, Duke T, Bullmore E. 2006. Adaptive reconfiguration of fractal small-world human brain functional networks. Proc Natl Acad Sci U S A. 103:19518-19523.

Behrens TE, Johansen-Berg H, Woolrich MW, Smith SM, Wheeler-Kingshott CA, Boulby PA, Barker GJ, Sillery EL, Sheehan K, Ciccarelli O. 2003. Non-invasive mapping of connections between human thalamus and cortex using diffusion imaging. Nat Neurosci. 6:750-757.

Bernasconi N, Bernasconi A, Caramanos Z, Antel SB, Andermann F, Arnold DL. 2003. Mesial temporal damage in temporal lobe epilepsy: a volumetric MRI study of the hippocampus, amygdala and parahippocampal region. Brain. 126:462-469.

Bernasconi N, Duchesne S, Janke A, Lerch J, Collins DL, Bernasconi A. 2004. Whole-brain voxel-based statistical analysis of gray matter and white matter in temporal lobe epilepsy. Neuroimage. 23:717-723.

Bernhardt BC, Bernasconi N, Concha L, Bernasconi A. 2010. Cortical thickness analysis in temporal lobe epilepsy: reproducibility and relation to outcome. Neurology. 74:1776-1784.

Bernhardt BC, Rozen DA, Worsley KJ, Evans AC, Bernasconi N, Bernasconi A. 2009. Thalamo-cortical network pathology in idiopathic generalized epilepsy: insights from MRI-based morphometric correlation analysis. Neuroimage. 46:373-381.

Bernhardt BC, Worsley KJ, Besson P, Concha L, Lerch JP, Evans AC, Bernasconi N. 2008. Mapping limbic network organization in temporal lobe epilepsy using morphometric correlations: insights on the relation between mesiotemporal connectivity and cortical atrophy. Neuroimage. 42:515-524.

Bernhardt BC, Worsley KJ, Kim H, Evans AC, Bernasconi A, Bernasconi N. 2009. Longitudinal and cross-sectional analysis of atrophy in pharmacoresistant temporal lobe epilepsy. Neurology. 72:1747-1754.

Bettus G, Guedj E, Joyeux F, Confort-Gouny S, Soulier E, Laguitton V, Cozzone PJ, Chauvel P, Ranjeva JP, Bartolomei F, et al. 2009. Decreased basal fMRI functional connectivity in epileptogenic networks and contralateral compensatory mechanisms. Hum Brain Mapp. 30:1580-1591.

Bonilha L, Rorden C, Castellano G, Pereira F, Rio PA, Cendes F, Li LM. 2004. Voxel-based morphometry reveals gray matter network atrophy in refractory medial temporal lobe epilepsy. Arch Neurol. 61:1379-1384.

Bullmore E, Sporns O. 2009. Complex brain networks: graph theoretical analysis of structural and functional systems. Nat Rev Neurosci. 10:186-198.

Bullmore ET, Suckling J, Overmeyer S, Rabe-Hesketh S, Taylor E, Brammer MJ. 1999. Global, voxel, and cluster tests, by theory and permutation, for a difference between two groups of structural MR images of the brain. IEEE Trans Med Imaging. 18:32-42.

Bullmore ET, Woodruff PW, Wright IC, Rabe-Hesketh S, Howard RJ, Shuriquie N, Murray RM. 1998. Does dysplasia cause anatomical dysconnectivity in schizophrenia? Schizophr Res. 30:127-135.

Cascino GD. 2009. Temporal lobe epilepsy is a progressive neurologic disorder: time means neurons! Neurology. 72:1718-1719.

Cascino GD, Jack CR, Jr, Parisi JE, Sharbrough FW, Hirschorn KA, Meyer FB, Marsh WR, O'Brien PC. 1991. Magnetic resonance imaging-based volume studies in temporal lobe epilepsy: pathological correlations. Ann Neurol. 30:31-36.

Chen ZJ, He Y, Rosa-Neto P, Germann J, Evans AC. 2008. Revealing modular architecture of human brain structural networks by using cortical thickness from MRI. Cereb Cortex. 18:2374-2381.

Cheverud JM. 1984. Quantitative genetics and developmental constraints on evolution by selection. J Theor Biol. 110:155-171.

Coan AC, Appenzeller S, Bonilha L, Li LM, Cendes F. 2009. Seizure frequency and lateralization affect progression of atrophy in temporal lobe epilepsy. Neurology. 73:834-842.

Collins DL, Holmes CJ, Peters TM, Evans AC. 1995. Automatic 3-D model-based neuroanatomical segmentation. Hum Brain Mapp. 3:190-208.

Collins DL, Neelin P, Peters TM, Evans AC. 1994. Automatic 3D intersubject registration of MR volumetric data in standardized Talairach space. J Comput Assist Tomogr. 18:192-205.

Concha L, Beaulieu C, Gross DW. 2005. Bilateral limbic diffusion abnormalities in unilateral temporal lobe epilepsy. Ann Neurol. 57:188-196.

Dabbs K, Jones J, Seidenberg M, Hermann B. 2009. Neuroanatomical correlates of cognitive phenotypes in temporal lobe epilepsy. Epilepsy Behav. 15:445-451.

Dauguet J, Peled S, Berezovskii V, Delzescaux T, Warfield SK, Born R, Westin CF. 2007. Comparison of fiber tracts derived from in-vivo DTI tractography with 3D histological neural tract tracer reconstruction on a macaque brain. Neuroimage. 37:530-538.

Dow C, Seidenberg M, Hermann B. 2004. Relationship between information processing speed in temporal lobe epilepsy and white matter volume. Epilepsy Behav. 5:919-925.

Dyhrfjeld-Johnsen J, Santhakumar V, Morgan RJ, Huerta R, Tsimring L, Soltesz I. 2007. Topological determinants of epileptogenesis in large-scale structural and functional models of the dentate gyrus derived from experimental data. J Neurophysiol. 97:1566-1587.

Engel J, Jr, Van Ness PC, Rasmussen T, Ojemann LM. 1993. Outcome with respect to epileptic seizures. In: Engel J, Jr, editor. Surgical treatment of the epilepsies. 2nd ed. New York: Raven. p. 609-621.

Freeman LC. 1977. Set of measures of centrality based on betweenness. Sociometry. 40:35-41.

Frings L, Schulze-Bonhage A, Spreer J, Wagner K. 2009. Remote effects of hippocampal damage on default network connectivity in the human brain. J Neurol. 256:2021-2029.

Friston KJ, Frith CD, Liddle PF, Frackowiak RS. 1993. Functional connectivity: the principal-component analysis of large (PET) data sets. J Cereb Blood Flow Metab. 13:5-14.

Girvan M, Newman ME. 2002. Community structure in social and biological networks. Proc Natl Acad Sci U S A. 99:7821-7826.

Gong G, He Y, Concha L, Lebel C, Gross DW, Evans AC, Beaulieu C. 2009. Mapping anatomical connectivity patterns of human cerebral cortex using in vivo diffusion tensor imaging tractography. Cereb Cortex. 19:524-536.

Guye M, Bettus G, Bartolomei F, Cozzone PJ. 2010. Graph theoretical analysis of structural and functional connectivity MRI in normal and pathological brain networks. MAGMA. 23:409-421.

Hagmann P, Cammoun L, Gigandet X, Meuli R, Honey CJ, Wedeen VJ, Sporns O. 2008. Mapping the structural core of human cerebral cortex. PLoS Biol. 6:e159.

He Y, Chen Z, Evans A. 2008. Structural insights into aberrant topological patterns of large-scale cortical networks in Alzheimer's disease. J Neurosci. 28:4756-4766.

He Y, Chen ZJ, Evans AC. 2007. Small-world anatomical networks in the human brain revealed by cortical thickness from MRI. Cereb Cortex. 17:2407-2419.

He Y, Dagher A, Chen Z, Charil A, Zijdenbos A, Worsley K, Evans A. 2009. Impaired small-world efficiency in structural cortical networks in multiple sclerosis associated with white matter lesion load. Brain. 132:3366-3379.

He Y, Wang J, Wang L, Chen ZJ, Yan C, Yang H, Tang H, Zhu C, Gong Q, Zang Y, et al. 2009. Uncovering intrinsic modular organization of spontaneous brain activity in humans. PLoS ONE. 4:e5226.

Hermann BP, Lin JJ, Jones JE, Seidenberg M. 2009. The emerging architecture of neuropsychological impairment in epilepsy. Neurol Clin. 27:881-907.

Horstmann MT, Bialonski S, Noennig N, Mai H, Prusseit J, Wellmer J, Hinrichs H, Lehnertz K. 2010. State dependent properties of epileptic brain networks: comparative graph-theoretical analyses of simultaneously recorded EEG and MEG. Clin Neurophysiol. 121:172-185.

Humphries MD, Gurney K. 2008. Network 'small-world-ness': a quantitative method for determining canonical network equivalence. PLoS ONE. 3:e0002051.

Humphries MD, Gurney K, Prescott TJ. 2006. The brainstem reticular formation is a small-world, not scale-free, network. Proc Biol Sci. 273:503-511.

Iturria-Medina Y, Sotero RC, Canales-Rodriguez EJ, Aleman-Gomez Y, Melie-Garcia L. 2008. Studying the human brain anatomical network via diffusion-weighted MRI and graph theory. Neuroimage. 40:1064-1076.

Johansen-Berg H, Behrens TE. 2006. Just pretty pictures? What diffusion tractography can add in clinical neuroscience. Curr Opin Neurol. 19:379-385.

Jokeit H, Ebner A. 1999. Long term effects of refractory temporal lobe epilepsy on cognitive abilities: a cross sectional study. J Neurol Neurosurg Psychiatry. 67:44-50.

Keller SS, Cresswell P, Denby C, Wieshmann U, Eldridge P, Baker G, Roberts N. 2007. Persistent seizures following left temporal lobe surgery are associated with posterior and bilateral structural and functional abnormalities. Epilepsy Res. 74:131-139.

Keller SS, Roberts N. 2008. Voxel-based morphometry of temporal lobe epilepsy: an introduction and review of the literature. Epilepsia. 49:741-757.

Kim JS, Singh V, Lee JK, Lerch J, Ad-Dab'bagh Y, MacDonald D, Lee JM, Kim SI, Evans AC. 2005. Automated 3-D extraction and evaluation of the inner and outer cortical surfaces using a Laplacian map and partial volume effect classification. Neuroimage. 27:210-221.

Kramer MA, Kolaczyk ED, Kirsch HE. 2008. Emergent network topology at seizure onset in humans. Epilepsy Res. 79:173-186.

Latora V, Marchiori M. 2001. Efficient behavior of small-world networks. Phys Rev Lett. 87:198701.

Lerch JP, Worsley K, Shaw WP, Greenstein DK, Lenroot RK, Giedd J, Evans AC. 2006. Mapping anatomical correlations across cerebral cortex (MACACC) using cortical thickness from MRI. Neuroimage. 31:993-1003.

Liao W, Zhang Z, Pan Z, Mantini D, Ding J, Duan X, Luo C, Lu G, Chen H. 2010. Altered functional connectivity and small-world in mesial temporal lobe epilepsy. PLoS ONE. 5:e8525.

MacDonald D, Kabani N, Avis D, Evans AC. 2000. Automated 3-D extraction of inner and outer surfaces of cerebral cortex from MRI. Neuroimage. 12:340-356.

Maslov S, Sneppen K. 2002. Specificity and stability in topology of protein networks. Science. 296:910-913.

Mazziotta JC, Woods R, Iacoboni M, Sicotte N, Yaden K, Tran M, Bean C, Kaplan J, Toga AW. 2009. The myth of the normal, average human brain—the ICBM experience: (1) subject screening and eligibility. Neuroimage. 44:914-922.

McDonald CR, Ahmadi ME, Hagler DJ, Tecoma ES, Iragui VJ, Gharapetian L, Dale AM, Halgren E. 2008. Diffusion tensor imaging correlates of memory and language impairments in temporal lobe epilepsy. Neurology. 71:1869-1876.

McDonald CR, Hagler DJ, Jr, Ahmadi ME, Tecoma E, Iragui V, Gharapetian L, Dale AM, Halgren E. 2008. Regional neocortical thinning in mesial temporal lobe epilepsy. Epilepsia. 49:794-803.

McMillan AB, Hermann BP, Johnson SC, Hansen RR, Seidenberg M, Meyerand ME. 2004. Voxel-based morphometry of unilateral temporal lobe epilepsy reveals abnormalities in cerebral white matter. Neuroimage. 23:167-174.

Meencke HJ, Veith G. 1991. Hippocampal sclerosis in epilepsy. In: Lüders H, editor. Epilepsy surgery. New York: Raven Press. p. 705-715.

Mesulam MM. 1998. From sensation to cognition. Brain. 121 (Pt 6):1013-1052.

Mitelman SA, Buchsbaum MS, Brickman AM, Shihabuddin L. 2005. Cortical intercorrelations of frontal area volumes in schizophrenia. Neuroimage. 27:753-770.

Netoff TI, Clewley R, Arno S, Keck T, White JA. 2004. Epilepsy in small-world networks. J Neurosci. 24:8075-8083.

Newman ME. 2003. The structure and function of complex networks. SIAM Rev Soc Ind Appl Math. 45:167-256.

Parent A, Carpenter MB. 1995. Human neuroanatomy. Baltimore (MD): Williams & Wilkins.

Parker GJ, Alexander DC. 2005. Probabilistic anatomical connectivity derived from the microscopic persistent angular structure of cerebral tissue. Philos Trans R Soc Lond B Biol Sci. 360:893–902.

Parker GJ, Stephan KE, Barker GJ, Rowe JB, MacManus DG, Wheeler-Kingshott CA, Ciccarelli O, Passingham RE, Spinks RL, Lemon RN, et al. 2002. Initial demonstration of in vivo tracing of axonal projections in the macaque brain and comparison with the human brain using diffusion tensor imaging and fast marching tractography. Neuroimage. 15:797–809.

Ponten SC, Bartolomei F, Stam CJ. 2007. Small-world networks and epilepsy: graph theoretical analysis of intracerebrally recorded mesial temporal lobe seizures. Clin Neurophysiol. 118:918–927.

Ponten SC, Douw L, Bartolomei F, Reijneveld JC, Stam CJ. 2009. Indications for network regularization during absence seizures: weighted and unweighted graph theoretical analyses. Exp Neurol. 217:197–204.

Powell HW, Parker GJ, Alexander DC, Symms MR, Boulby PA, Wheeler-Kingshott CA, Barker GJ, Koepp MJ, Duncan JS. 2007. Abnormalities of language networks in temporal lobe epilepsy. Neuroimage. 36:209–221.

Ryvlin P. 2003. Beyond pharmacotherapy: surgical management. Epilepsia. 44(Suppl 5):23–28.

Salvador R, Suckling J, Coleman MR, Pickard JD, Menon D, Bullmore E. 2005. Neurophysiological architecture of functional magnetic resonance images of human brain. Cereb Cortex. 15:1332–1342.

Schindler KA, Bialonski S, Horstmann MT, Elger CE, Lehnertz K. 2008. Evolving functional network properties and synchronizability during human epileptic seizures. Chaos. 18:033119.

Seidenberg M, Kelly KG, Parrish J, Geary E, Dow C, Rutecki P, Hermann B. 2005. Ipsilateral and contralateral MRI volumetric abnormalities in chronic unilateral temporal lobe epilepsy and their clinical correlates. Epilepsia. 46:420–430.

Sled JG, Zijdenbos AP, Evans AC. 1998. A nonparametric method for automatic correction of intensity nonuniformity in MRI data. IEEE Trans Med Imaging. 17:87–97.

Sporns O, Chialvo DR, Kaiser M, Hilgetag CC. 2004. Organization, development and function of complex brain networks. Trends Cogn Sci. 8:418–425.

Sporns O, Zwi JD. 2004. The small world of the cerebral cortex. Neuroinformatics. 2:145–162.

Stam CJ. 2004. Functional connectivity patterns of human magneto-encephalographic recordings: a 'small-world' network? Neurosci Lett. 355:25–28.

Sutula TP, Hagen J, Pitkanen A. 2003. Do epileptic seizures damage the brain? Curr Opin Neurol. 16:189–195.

Theodore WH, Gaillard WD. 2002. Neuroimaging and the progression of epilepsy. In: Sutula T, Pitkanen A, editors. Do seizures damage the brain. The Netherlands: Elsevier Amsterdam. p. 305–313.

Tzourio-Mazoyer N, Landeau B, Papathanassiou D, Crivello F, Etard O, Delcroix N, Mazoyer B, Joliot M. 2002. Automated anatomical labeling of activations in SPM using a macroscopic anatomical parcellation of the MNI MRI single-subject brain. Neuroimage. 15:273–289.

van Dellen E, Douw L, Baayen JC, Heimans JJ, Ponten SC, Vandertop WP, Velis DN, Stam CJ, Reijneveld JC. 2009. Long-term effects of temporal lobe epilepsy on local neural networks: a graph theoretical analysis of corticography recordings. PLoS ONE. 4:e8081.

Voets NL, Adcock JE, Stacey R, Hart Y, Carpenter K, Matthews PM, Beckmann CF. 2009. Functional and structural changes in the memory network associated with left temporal lobe epilepsy. Hum Brain Mapp. 30:4070–4081.

Waites AB, Briellmann RS, Saling MM, Abbott DF, Jackson GD. 2006. Functional connectivity networks are disrupted in left temporal lobe epilepsy. Ann Neurol. 59:335–343.

Watts DJ, Strogatz SH. 1998. Collective dynamics of 'small-world' networks. Nature. 393:440–442.

Wright IC, Sharma T, Ellison ZR, McGuire PK, Friston KJ, Brammer MJ, Murray RM, Bullmore ET. 1999. Supra-regional brain systems and the neuropathology of schizophrenia. Cereb Cortex. 9:366–378.

Yogarajah M, Duncan JS. 2008. Diffusion-based magnetic resonance imaging and tractography in epilepsy. Epilepsia. 49:189–200.

Zhang K, Sejnowski TJ. 2000. A universal scaling law between gray matter and white matter of cerebral cortex. Proc Natl Acad Sci U S A. 97:5621–5626.